Financial Statistical Journal 2024, 7(2), 9177.
https://doi.org/10.24294/fsj9177

Article

A novel circular dynamics in financial networks with cross-correlated volatility and asset movements

Subhrajit Saha, Debashis Chatterjee*

Department of Statistics, Siksha Bhavana (Institution of Science), Visva Bharati, Bolpur, Santiniketan 731235, India
*** Corresponding author:** Debashis Chatterjee, debashis.chatterjee@visva-bharati.ac.in

CITATION

Saha S, Chatterjee D. A novel circular dynamics in financial networks with cross-correlated volatility and asset movements. Financial Statistical Journal. 2024; 7(2): 9177. https://doi.org/10.24294/fsj9177

ARTICLE INFO

Received: 18 September 2024
Accepted: 6 December 2024
Available online: 16 December 2024

Abstract: In this paper, we propose a novel application of classical directional statistics to model the cross-correlation of asset volatility in financial networks. The proposed novel Circular Volatility Model (CVM) provides a framework for studying the interdependencies of financial assets whose returns exhibit periodic behaviors. By extending traditional volatility models into a circular framework, we establish new pathways for understanding the cyclicity inherent in market dynamics. Our model is rigorously grounded in classical \& directional statistics, utilizing von Mises distributions for parameter estimation and novel circular covariance structures. We offer formal derivations, maximum likelihood estimates, and a novel goodness-of-fit testing framework for this circular model. We establish our methodologies using simulation studies.

Keywords: circular volatility model; von mises distribution; angular data; financial networks; volatility modeling; Maximum Likelihood Estimation (MLE); confidence intervals

1. Introduction

In financial markets, asset returns frequently exhibit cyclic behaviors influenced by market sentiment, external shocks, and cyclical economic conditions. Traditional linear models fail to account for the periodic nature of such phenomena. In contrast, circular statistics allow us to model returns and volatility within a framework that respects their angular nature. This paper introduces the Circular Volatility Model (CVM), which extends the GARCH volatility models into the circular domain. The CVM utilizes von Mises distributions for angular data and incorporates circular cross-correlations between assets in a financial network.

2. Related works

The dynamics of financial networks, particularly in the context of cross-correlated volatility and asset movements, have garnered significant attention in recent years. A growing body of literature has explored the interconnectedness of financial markets and the implications of this interconnectedness for systemic risk and volatility spillovers.

Addresses modeling and analyzing time series of unit two-dimensional vectors, evaluating multiple model classes for feasibility, and recommends a dual-class approach using standard time series algorithms, applied to wind direction data analysis [1].

Explores modeling and analyzing time series of unit two-dimensional vectors, recommends a dual-class approach using standard time series algorithms, and demonstrates its application to wind direction data [2].

Develops the MF-APCCA method to analyze asymmetric risk transmission between cryptocurrencies and global stock markets, showing stronger cross-correlations between Bitcoin and G7 markets than with E7 markets, with gold providing risk-buffering effects [3].

Examines dynamic risk resonance across Chinese market sectors, finding time-varying effects with transportation and utilities as net transmitters, low-frequency events exerting prolonged impact, and crises amplifying resonance [4].

Uses time and frequency connectedness methods to analyze volatility links between 27 emerging markets and seven major cryptocurrencies, finding increased global risk spillovers post-COVID-19, with key risk transmitters and limited diversification benefits for emerging market portfolios [5].

Uses asymmetric multifractal cross-correlation analysis to reveal that gold is the most efficient asset, with green stocks as net transmitters of shocks and halal tourism stocks and oil as net receivers, while a minimum connectedness portfolio offers strong hedging benefits during major economic events [6].

Uses spillover index and wavelet approaches to analyze multiscale relationships among major cryptocurrencies, finding Monero as a key risk transmitter and Ethereum as the main receiver, with enhanced diversification benefits at lower scales in mixed portfolios [7].

Applies a DCC-GARCH model to analyze volatility connectedness among major cryptocurrencies, revealing that low investor sentiment correlates with heightened market connectedness and volatility, while high sentiment supports greater diversification [8].

Examines cryptocurrency integration and contagion during the COVID-19 pandemic, finding mixed integration levels and no contagion, suggesting cryptocurrencies could serve as a good investment during global shocks [9].

Applies artificial neural networks to predict Bitcoin price trends using symmetric volatility attributes, finding high accuracy and identifying the low price as the primary driver for price predictions [10].

Explores volatility spillovers between crude oil prices and cryptocurrencies, finding bidirectional spillovers between oil and Bitcoin, and unidirectional spillovers from oil to Bitcoin Cash and from cryptocurrencies like Ethereum to oil [11].

Suggests inefficiency in the Brazilian stock market, evidenced by strong long-term cross-correlations with foreign markets, fat-tailed log-returns, and successful predictions of IBOVESPA futures using a neural network model [12].

One of the foundational works in this area is by [13], who developed an analytical model to understand contagion in financial networks. They demonstrated that the network's structure significantly influences the probability and impact of contagion, highlighting a robust yet fragile characteristic of financial systems where low probabilities of contagion can lead to widespread effects during crises.

This notion is echoed in the work of [14], who emphasize the importance of understanding financial interdependencies to mitigate systemic risks. Their model illustrates how organizations' values are interlinked through various financial instruments, which can exacerbate the effects of shocks across the network. This approach complements the work of [14], who drew parallels between financial

networks and ecological systems, suggesting that complexity can lead to systemic vulnerabilities.

The COVID-19 pandemic has further illuminated the dynamics of financial networks [15] analyzed the connectedness among stock markets during this period, providing a visualization of pandemic risk that parallels financial risk. Their findings suggest that the degree of connectedness can serve as a critical indicator of systemic risk, reinforcing the need for robust network analysis in understanding financial contagion.

Similarly, [16] employed a GARCH model to assess risk spillovers between crude oil and stock markets during the pandemic, revealing complex interdependencies that traditional methods may overlook.

Research on volatility spillovers has also gained traction, particularly in commodity markets. [17] identified a significant shift in the correlation structure between commodities and stock markets post-2008 financial crisis, indicating that financialization has led to increased risk spillovers.

Supports this [18] who found that stock market shocks have a pronounced impact on agricultural commodity price volatility, particularly following major financial disruptions. Their work underscores the growing integration between financial and commodity markets, which complicates the dynamics of volatility transmission.

The role of uncertainty in financial markets has been another focal point of research. [19] highlighted that uncertainty is a central node in the volatility transmission network, influencing spillovers among various financial markets.

This aligns with the findings of [20], who explored the interdependence of financial markets in South and East Asia, revealing that economic shocks can propagate across borders through volatility transmission.

Moreover, the methodological advancements in analyzing financial networks have contributed to a deeper understanding of these dynamics. [21] introduced a metapopulation network model to study the spreading of financial risk, emphasizing the importance of network structure in understanding risk dynamics. The literature on financial networks reveals a complex interplay of interconnectedness, volatility spillovers, and systemic risk. The insights gained from these studies underscore the necessity for comprehensive models that account for the dynamic nature of financial interdependencies. As financial markets continue to evolve, ongoing research will be essential to navigate the challenges posed by these interconnected systems.

The Circular Volatility Model (CVM) proposed in this paper builds upon classical and circular statistical frameworks, particularly the von Mises distribution, which is pivotal in modeling circular data. The von Mises distribution has been extensively utilized in various fields, including bioinformatics and directional data analysis, due to its ability to capture the cyclic nature of phenomena [22] and [23].

For instance, [23] highlighted the fundamental properties of multivariate von Mises distributions, establishing a foundation for analyzing directional data directly applicable to financial asset returns that exhibit periodic behaviors.

In financial markets, herd behavior has been a focal point in understanding volatility interdependencies. [24] provided empirical evidence of herd behavior across global stock markets, indicating that asset returns often move in tandem during periods of high volatility. This phenomenon aligns with the cyclicity that we aim to model in

this paper, as it reflects the collective behavior of investors, which can lead to synchronized fluctuations in asset prices.

Similarly, [25] explored the implications of foreign institutional herding in the Taiwanese stock market, further supporting the notion that market dynamics are influenced by collective investor behavior.

The theoretical underpinnings of the CVM are further supported by advancements in statistical methodologies for directional data. For instance, [26] emphasized the importance of the von Mises distribution in antenna design, showcasing its versatility in modeling directional phenomena. This adaptability is mirrored in financial applications, where asset returns' cyclic nature necessitates a similar modeling approach.

This research offers a novel methodology for analyzing cyclical behaviors in asset returns and volatilities, with rigorous mathematical foundations and wide applicability in finance.

3. Objective and novelty of the research

The primary objective of this research is to develop a rigorous and mathematically sophisticated model that captures the directional dependencies between asset returns and volatilities in financial markets. Unlike traditional multivariate models that operate in a linear space, our model addresses the periodicity of financial data. The novelty of this research lies in:

- Extending the classical GARCH model into the circular domain.
- Introducing a new circular cross-correlation measure that captures the angular dependencies between assets.
- Proposing a novel goodness-of-fit test for circular data.
- Establishing formal parameter estimation techniques using von Mises distributions.

The Circular Volatility Model (CVM) extends the traditional GARCH framework into the circular domain, effectively capturing the periodic and directional dependencies inherent in financial asset returns. Through rigorous mathematical formulation and establishing key statistical properties, the CVM provides a robust tool for modeling and analyzing volatility in complex financial networks. This novel application of directional statistics to financial markets opens new avenues for understanding asset dependencies in complex financial networks.

4. Preliminaries

4.1. Circular statistics

Circular statistics is a branch of statistics that deals with data measured in angles or directions. Let $\theta \in [0,2\pi)$ represent a circular variable, such as the direction of a return in a financial asset. In contrast to linear data, the distance between two angles is not Euclidean. For example, the distance between $350°$ and $10°$ is $20°$, not $340°$. Circular data must be analyzed using specialized techniques, such as the von Mises distribution, which is the circular analog of the normal distribution.

4.2. Von mises distribution

The von Mises distribution is given by:

$$f(\theta;\mu,\kappa) = \frac{e^{\kappa\cos(\theta-\mu)}}{2\pi I_0(\kappa)}$$

where μ is the mean direction, κ is the concentration parameter, and $I_0(\kappa)$ is the modified Bessel function of the first kind. This distribution is used extensively in the modeling of angular data because it captures the periodicity inherent in circular variables.

4.3. GARCH model for volatility

The Generalized Autoregressive Conditional Heteroskedasticity (GARCH) model, introduced by Bollerslev [27], is a cornerstone in modeling financial time series volatility. The GARCH (1,1) model, in its simplest form, is defined as:

$$\sigma_t^2 = \alpha_0 + \alpha_1\epsilon_{t-1}^2 + \beta_1\sigma_{t-1}^2 \quad (1)$$

where:

- σ_t^2 is the conditional variance (volatility) at time t.
- $\alpha_0 > 0$ is the constant term.
- $\alpha_1 \geq 0$ measures the reaction of volatility to past shocks (ARCH term).
- $\beta_1 \geq 0$ captures the persistence of volatility (GARCH term).
- $\epsilon_t = r_t - \mu_t$ is the residual or shock at time r_t where μ_t is the return and μt is the mean return.

The GARCH (1,1) model effectively captures the volatility clustering observed in financial time series, where high-volatility periods tend to cluster together, as do low-volatility periods.

5. Circular volatility model (CVM)

5.1. Motivation for circular volatility modeling

Traditional GARCH models operate within a linear framework, assuming that returns and volatilities evolve over a linear time scale. However, financial markets exhibit periodic and cyclical behaviors influenced by various factors such as trading hours, economic cycles, and seasonal effects. To capture these cyclical dynamics, it is advantageous to extend the GARCH framework into the circular domain, where angular dependencies can be explicitly modeled.

Circular data, characterized by angles or directions, naturally encapsulate periodicity and cyclicity. For instance, intra-day trading patterns may exhibit regular cycles corresponding to market opening and closing times. By incorporating circular distance into the GARCH model, we can better model and understand the directional dependencies and cyclical behaviors inherent in financial data.

5.2. Model definition

The Circular Volatility Model (CVM) is designed to extend the traditional GARCH (1,1) model into the circular domain, where asset returns are treated as

angular data. This is crucial when dealing with financial systems where periodicity and cyclic behaviors are present, such as intra-day or quarterly trading cycles. The CVM introduces angular cross-correlations between asset volatilities to capture these cyclical patterns more accurately. Let $\{\theta_i(t)\}_{t\in Z}$ denote the sequence of angular returns for asset *i*, where $\theta_i(t) \in [0,2\pi)$. The CVM for asset *i* is defined by the following recursive equation:

$$\sigma_i^2(t) = \alpha_0 + \alpha_1 \sum_{j=1}^{N} w_{ij} \cos\left(\theta_i(t) - \theta_j(t)\right) + \beta_1 \sigma_i^2(t-1) \quad (2)$$

where:

- $\sigma_i^2(t)$ is the conditional variance (volatility) of asset *i* at time *t*.
- $\alpha_0 > 0$ is the intercept term, representing the baseline level of volatility.
- $\alpha_1 \geq 0$ captures the influence of the angular cross-correlations between asset *i* and all other assets *j* = 1, 2, ..., *N*.
- $\beta_1 \geq 0$ is the autoregressive parameter, reflecting the persistence of volatility over time.
- $w_{ij} \geq 0$ are weights representing the influence of asset *j* on asset *i*, satisfying the
- normalization condition $\sum_{j=1}^{N} w_{ij} = 1$
- $cos\left(\theta_i(t) - \theta_j(t)\right)$ captures the circular (angular) correlation between the returns of assets *i* and *j*.
- $\theta_i(t) \sim$ von Mises (μ_i, κ_i), indicating that the angular returns follow a von Mises distribution with mean direction μ_i and concentration parameter κ_i.

The incorporation of circular distance $\Delta_{ij}(t)$ into the GARCH framework allows the model to account for the directional alignment between different assets. Unlike the traditional GARCH model, which considers only the magnitude of past shocks, the CGARCH model integrates directional information, thereby enriching the volatility dynamics with cyclical dependencies.

5.3. Interpretation of model components

The term $\cos\left(\theta_i(t) - \theta_j(t)\right)$ measures the alignment between the directional returns of assets *i* and *j*. A value close to 1 implies that the assets are moving in the same direction, thus contributing positively to the volatility of asset *i*. Conversely, a value near −1 indicates opposing directions, potentially reducing the volatility contribution.

The weights w_{ij} allow for differential influences of various assets on asset *i*, enabling the model to capture complex interdependencies within the financial network.

Consider two assets, A and B, with angular returns $\theta_A(t)$ and $\theta_B(t)$. If their angular difference $\theta_A(t) - \theta_B(t)$ is close to zero, it implies that these assets are moving in a synchronized manner, increasing the volatility of asset A due to a positive correlation.

If the angular difference is close to π, the assets move in opposite directions, contributing less to the overall volatility. The periodic cosine function handles these variations effectively.

The parameters α_0, α_1, β_1, μ_i, and κ_i provide valuable insights into the behavior of asset volatilities:

1) α0 reflects the baseline volatility level, independent of cross-asset interactions.
2) α1 captures the impact of angular cross-correlations, revealing how much the angular returns of other assets influence the volatility of an asset.
3) β1 indicates the persistence of volatility over time, similar to the autoregressive term in the traditional GARCH model.
4) μ_i and κ_i describe the distribution of angular returns, where μ_i represents the average direction and κ_i represents the concentration of returns around this direction.

These insights are essential for portfolio optimization and risk management, especially when assets exhibit periodic or cyclical behaviors.

6. Parameter estimation using maximum likelihood estimation (MLE)

To estimate the parameters of the Circular Volatility Model (CVM), we employ the Maximum Likelihood Estimation (MLE) method. The MLE process enables us to derive parameter estimates that maximize the likelihood of the observed data under the proposed model.

6.1. Model specification

In the Circular Volatility Model, the observed angular returns for asset *i* at time *t*, denoted by $\theta_i(t) \in [0,2\pi)$, follow a Von Mises distribution with mean direction μ_i and concentration parameter κ_i. The conditional variance $\sigma_i^2(t)$ for each asset *i* is governed by the GARCH (1,1) structure extended into the circular domain:

$$\sigma_i^2(t) = \alpha_0 + \alpha_1 \sum_{j=1}^{N} w_{ij} \cos\left(\theta_i(t) - \theta_j(t)\right) + \beta_1 \sigma_i^2(t-1) \tag{3}$$

where:

- $\alpha_0 > 0$ is the baseline level of volatility.
- $\alpha_1 \geq 0$ quantifies the effect of angular cross-correlations with other assets.
- $\beta_1 \geq 0$ represents the autoregressive effect of past volatility.
- $w_{ij} \geq 0$ are weights for the influence of asset *j* on asset *i*.

6.2. Likelihood function construction

The probability density function (PDF) of the von Mises distribution for each angular return $\theta_i(t)$ is:

$$f(\theta_i(t); \mu_i, \kappa_i) = \frac{e^{\kappa_i \cos(\theta_i(t) - \mu_i)}}{2\pi I_0(\kappa_i)} \tag{4}$$

where:

1) μ_i is the mean direction for asset *i*.
2) κ_i is the concentration parameter, analogous to the precision of the distribution.

3) $I_0(\kappa_i)$ is the modified Bessel function of the first kind, serving as a normalization factor.

Given observed data $\theta_i(t)\}_{t=1}^{T}$for each asset *i* and time period *T*, the likelihood function for the CVM is constructed as the product of the individual probabilities for each $\theta_i(t)$:

$$L(\alpha_0, \alpha_1, \beta_1, \{\mu_i\}, \{\kappa_i\}) = \prod_{i=1}^{N} \prod_{t=1}^{T} f(\theta_i(t); \mu_i, \kappa_i) \tag{5}$$

6.3. Log-likelihood function

To facilitate maximization, we take the natural logarithm of the likelihood function, yielding the log-likelihood function:

$$\mathcal{L}(\alpha_0, \alpha_1, \beta_1, \{\mu_i\}, \{\kappa_i\}) = \sum_{i=1}^{N} \sum_{t=1}^{T} \left(\kappa_i \cos(\theta_i(t) - \mu_i) - \log\left(2\pi I_0(\kappa_i)\right)\right) \tag{6}$$

Maximizing this log-likelihood with respect to α_0, α_1, β_1, μ_i, and κ_i yields the MLE estimates for these parameters.

6.4. Step-by-step MLE process

To obtain the MLEs, we differentiate the log-likelihood function with respect to each parameter, set the derivatives equal to zero, and solve the resulting equations.

Differentiation with Respect to μ_i

The partial derivative of $\mathcal{L}$ with respect to μ_i for each asset *i* is:

$$\frac{\partial \mathcal{L}}{\partial \mu_i} = \sum_{t=1}^{T} \kappa_i \sin(\theta_i(t) - \mu_i) \tag{7}$$

Setting $\frac{\partial \mathcal{L}}{\partial \mu_i} = 0$ gives:

$$\sum_{t=1}^{T} \sin(\theta_i(t) - \mu_i) = 0 \tag{8}$$

This equation can be solved numerically to obtain the MLE $\hat{\mu}_i$ for each asset *i*.

Differentiation with Respect to κ_i

The partial derivative of $\mathcal{L}$ with respect to κ_i is

$$\frac{\partial \mathcal{L}}{\partial \kappa_i} = \sum_{t=1}^{T} \left(\cos(\theta_i(t) - \mu_i) - \frac{I_1(\kappa_i)}{I_0(\kappa_i)}\right) \tag{9}$$

where $I_1(\kappa_i)$ is the modified Bessel function of the first kind of order 1. Setting $\frac{\partial \mathcal{L}}{\partial \kappa_i} = 0$ gives:

$$\sum_{t=1}^{T} \cos(\theta_i(t) - \mu_i) = T \frac{I_1(\kappa_i)}{I_0(\kappa_i)} \tag{10}$$

Solving this equation numerically provides the MLE κ_i.

Differentiation with Respect to $\alpha_0, \alpha_1 \; and \; \beta_1$

For the parameters $\alpha_0, \alpha_1 \; and \; \beta_1$ in the volatility equation, we use iterative methods to find the estimates. Given the recursive structure of $\sigma_i^2(t)$, we calculate the partial derivatives of $\mathcal{L}$ with respect to these parameters, which involve the chain rule and the autoregressive terms.

- Differentiation with respect to α_0:

$$\frac{\partial \mathcal{L}}{\partial \alpha_0} = \sum_{i=1}^{N} \sum_{t=1}^{T} \frac{\partial \sigma_i^2(t)}{\partial \alpha_0} \tag{11}$$

- Differentiation with respect to α_1:

$$\frac{\partial \mathcal{L}}{\partial \alpha_1} = \sum_{i=1}^{N} \sum_{t=1}^{T} \sum_{j=1}^{N} w_{ij} \frac{\partial \, cos\left(\theta_i(t) - \theta_j(t)\right)}{\partial \alpha_1} \tag{12}$$

- Differentiation with respect to β_1:

$$\frac{\partial \mathcal{L}}{\partial \beta_1} = \sum_{i=1}^{N} \sum_{t=1}^{T} \frac{\partial \sigma_i^2(t-1)}{\partial \beta_1} \tag{13}$$

These derivatives do not have closed-form solutions, so we use numerical optimization techniques, such as the Newton-Raphson or Expectation-Maximization (EM) algorithm, to obtain the MLE estimates $\widehat{\alpha_0}, \widehat{\alpha_1}, and \; \widehat{\beta_1}$.

6.5. Numerical optimization

Given the recursive nature of $\sigma_i^2(t)$ and the nonlinear relationship between parameters, numerical optimization methods are essential for solving the MLE equations. We employ an iterative algorithm that alternates between updating $\{\mu_i\}$, $\{\kappa_i\}$, α_0, α_1, and β_1, with the following steps:

(1) Initialize α_0, α_1, β_1, $\{\mu_i\}$ and $\{\kappa_i\}$ with reasonable starting values.

(2) Calculate the conditional variances $\sigma_i^2(t)$ using the current parameter estimates.

(3) Update each parameter by maximizing the log-likelihood with respect to that parameter while holding the others fixed.

(4) Repeat steps 2–3 until convergence, i.e., until changes in parameter estimates fall below a predefined threshold.

This approach yields the final MLE estimates $\widehat{\alpha_0}, \widehat{\alpha_1}, \widehat{\beta_1}, \{\widehat{\mu_i}\}, and \; \{\widehat{\kappa_i}\}$.

6.6. Interpretation of estimated parameters

Once estimated, these parameters provide insights into the behavior of volatility and directional dependencies in the financial network:

- $\widehat{\alpha_0}$: Baseline level of volatility.
- $\widehat{\alpha_1}$: Influence of angular cross-correlations on volatility.
- $\widehat{\beta_1}$: Persistence of volatility over time.
- $\widehat{\mu_i}$: Average directional return of asset *i*.

- $\widehat{\kappa_i}$: Concentration of angular returns around $\widehat{\mu_i}$, indicating the variability in directional movement.

Together, these estimates enable a comprehensive understanding of the dynamics within circular financial data.

7. Stationarity conditions for CVM

This section provides a rigorous mathematical answer for the stationarity condition of the Circular Volatility Model (CVM). The CVM extends the traditional GARCH (1,1) model into the circular domain, accommodating the periodic nature of financial asset returns. This formal definition ensures clarity and lays the foundation for subsequent theoretical properties and estimations. For details of circular time series, we refer to [2] and [28].

Theorem 1. *(Stationarity of CVM). If the Circular Volatility Model (CVM) defined in Equation (3) is strictly stationary, then* $\beta_1 < 1$ *and* $\alpha_1 \cdot \lambda_{max}(W) + \beta_1 < 1$ *here* $\lambda_{max}(W)$ *is the maximum eigenvalue of the weight matrix* $W = [w_{ij}]$.

Proof of Theorem 1. To establish the stationarity of the CVM, we examine the conditions under which the model's conditional variance $\sigma_i^2(t)$ remains stable over time.

Expectation of the CVM Equation:

Taking expectations on both sides of Equation (3), we have:

$$E[\sigma_i^2(t)] = \alpha_0 + \alpha_1 \sum_{j=1}^{N} w_{ij} E\left[\cos\left(\theta_i(t) - \theta_j(t)\right)\right] + \beta_1 E[\sigma_i^2(t-1)]$$

Stationarity Assumption:

Assume that the process is strictly stationary, implying

$$E[\sigma_i^2(t)] = E[\sigma_i^2(t-1)] = \sigma_i^2$$

Substituting into the above equation:

$$\sigma_i^2 = \alpha_0 + \alpha_1 \sum_{j=1}^{N} w_{ij} E\left[\cos\left(\theta_i(t) - \theta_j(t)\right)\right] + \beta_1 \sigma_i^2$$

Solving for σ_i^2:

Rearranging terms:

$$\sigma_i^2(1-\beta_1) = \alpha_0 + \alpha_1 \sum_{j=1}^{N} w_{ij} E\left[\cos\left(\theta_i(t) - \theta_j(t)\right)\right]$$

Therefore:

$$\sigma_i^2 = \frac{\alpha_0 + \alpha_1 \sum_{j=1}^{N} w_{ij} E\left[\cos\left(\theta_i(t) - \theta_j(t)\right)\right]}{(1-\beta_1)}$$

Ensuring Positive Variance:

For σ_i^2 to be positive and finite, the denominator must satisfy $1 - \beta_1 > 0, i.e., \beta_1 < 1$.

Boundedness of the Cosine Expectation:

The expectation $E\left[\cos\left(\theta_i(t) - \theta_j(t)\right)\right]$ is bounded between −1 and 1. Therefore:

$$-\alpha_1 \times \sum_{j=1}^{N} w_{ij} \leq \alpha_1 \sum_{j=1}^{N} w_{ij} E\left[\cos\left(\theta_i(t) - \theta_j(t)\right)\right] \leq \alpha_1 \times \sum_{j=1}^{N} w_{ij}$$

Given that $\sum_{j=1}^{N} w_{ij} = 1$:

$$-\alpha_1 \leq \alpha_1 \sum_{j=1}^{N} w_{ij} E\left[\cos\left(\theta_i(t) - \theta_j(t)\right)\right] \leq \alpha_1$$

Eigenvalue Condition:

To ensure that the impact of the cross-correlations does not destabilize the volatility process, we impose:

$$\alpha_1 \times \lambda_{\max}(W) + \beta_1 < 1$$

where $\lambda_{max}(W)$ is the largest eigenvalue of the weight matrix W. This condition guarantees that the combined influence of cross-correlations and volatility persistence is controlled, ensuring stationarity.

Under the condition $\alpha_1 \times \lambda_{max}(W) + \beta_1 < 1$, the CVM maintains a stable conditional variance, thereby satisfying the criteria for strict stationarity. □

8. Circular covariance structure

In this section, we introduce the novel concept of a circular covariance matrix to model the interdependencies between angular returns of financial assets. In traditional linear statistics, covariance measures how two variables change together. However, when dealing with circular data, such as angles or periodic variables, the standard definition of covariance must be adapted to account for the wrapping nature of the data, where angles $0°$ and $360°$ represent the same point on a circle. Hence, the circular covariance must capture both the angular relationships and the periodicity inherent in such data.

Let $\theta_i(t)$ and $\theta_j(t)$ represent the angular returns of assets i and j at time t, where $\theta_i, \theta_j \in [0,2\pi)$. The covariance between two angular returns can be expressed as a function of their directional differences. For assets i and j, the circular covariance structure is defined as:

$$\Sigma_{\theta_{ij}} = \kappa_i \kappa_j \cos\left(\mu_i - \mu_j\right)$$

where:

- κ_i and κ_j are the concentration parameters (analogous to precision) of the von Mises distributions fitted to $\theta_i(t)$ and $\theta_j(t)$, respectively.
- μ_i and μ_j are the mean directions of the angular returns for assets i and j.

The circular covariance matrix Σ_θ for N assets is thus given by:

$$\Sigma_\theta = \begin{pmatrix} \kappa_1^2 & \kappa_1\kappa_2\cos(\mu_1-\mu_2) & \cdots & \kappa_1\kappa_N\cos(\mu_1-\mu_N) \\ \kappa_2\kappa_1\cos(\mu_2-\mu_1) & \kappa_2^2 & \cdots & \kappa_2\kappa_N\cos(\mu_2-\mu_N) \\ \vdots & \vdots & \ddots & \vdots \\ \kappa_N\kappa_1\cos(\mu_N-\mu_1) & \kappa_N\kappa_2\cos(\mu_N-\mu_2) & \cdots & \kappa_N^2 \end{pmatrix}$$

Consider a simple example of $N = 3$ assets. Let the mean directions of the angular returns for assets 1, 2, and 3 be $\mu_1 = \frac{\pi}{4}$, $\mu_2 = \frac{\pi}{2}$ and $\mu_3 = \frac{3\pi}{4}$ respectively. Furthermore, assume the concentration parameters are $\kappa_1 = 2$, $\kappa_2 = 3$, and $\kappa_3 = 4$. The circular covariance matrix Σ_θ would be:

$$\Sigma_\theta = \begin{pmatrix} 4 & 6\cos\left(\frac{\pi}{4}-\frac{\pi}{2}\right) & 8\cos\left(\frac{\pi}{4}-\frac{3\pi}{4}\right) \\ 6\cos\left(\frac{\pi}{2}-\frac{\pi}{4}\right) & 9 & 12\cos\left(\frac{\pi}{2}-\frac{3\pi}{4}\right) \\ 8\cos\left(\frac{3\pi}{4}-\frac{\pi}{4}\right) & 12\cos\left(\frac{3\pi}{4}-\frac{\pi}{2}\right) & 16 \end{pmatrix}$$

Simplifying the trigonometric terms, we get:

$$\Sigma_\theta = \begin{pmatrix} 4 & 6\cos\left(-\frac{\pi}{4}\right) & 8\cos\left(-\frac{\pi}{2}\right) \\ 6\cos\left(\frac{\pi}{4}\right) & 9 & 12\cos\left(-\frac{\pi}{4}\right) \\ 8\cos\left(\frac{\pi}{2}\right) & 12\cos\left(\frac{\pi}{4}\right) & 16 \end{pmatrix}$$

Given that $\cos(-\theta) = \cos(\theta)$, we can substitute the cosine values to obtain:

$$\Sigma_\theta = \begin{pmatrix} 4 & 6\times\frac{\sqrt{2}}{2} & 8\cdot 0 \\ 6\times\frac{\sqrt{2}}{2} & 9 & 12\times\frac{\sqrt{2}}{2} \\ 8\times 0 & 12\times\frac{\sqrt{2}}{2} & 16 \end{pmatrix} = \begin{pmatrix} 4 & 3\sqrt{2} & 0 \\ 3\sqrt{2} & 9 & 6\sqrt{2} \\ 0 & 6\sqrt{2} & 16 \end{pmatrix}$$

This matrix fully represents the circular dependencies between the three assets. It is evident that the correlation between assets 1 and 3, for example, is zero because the angular separation between them is $\frac{\pi}{2}$, which corresponds to orthogonal directions.

8.1. Properties of the circular covariance matrix

The circular covariance matrix Σ_θ is a fundamental structure for modeling the dependencies between angular variables in a financial network. Unlike traditional covariance matrices, Σ_θ captures the specific properties of circular data, making it essential for accurate modeling in systems where periodicity is inherent, such as in asset returns that exhibit cyclical behavior. In this section, we elaborate on the key properties of Σ_θ and provide context-specific insights into its relevance in financial applications.

8.1.1. Symmetry

The circular covariance matrix Σ_θ retains the symmetry property, a characteristic shared with traditional covariance matrices. For assets i and j, the covariance between their angular returns is determined by:

$$\Sigma_{\theta_{ij}} = \kappa_i \kappa_j \cos(\mu_i - \mu_j)$$

where κ_i and κ_j represent the concentration parameters of the von Mises distribution fitted to the angular returns θ_i and θ_j, and $\mu_i$and μ_j are their mean directions.

Since the cosine function is symmetric, meaning that:

$$\cos(\theta_i - \theta_j) = \cos(\theta_j - \theta_i)$$

it follows that:

$$\Sigma_{\theta_{ij}} = \Sigma_{\theta_{ji}}$$

Thus, Σ_θ is a symmetric matrix. This symmetry ensures that the relationships between pairs of assets are consistently captured, and this is crucial in financial systems where reciprocal dependencies between asset volatilities are common.

8.1.2. Periodicity

The periodic nature of circular data is one of its defining features, and this is reflected in the covariance structure. The cosine function, $\cos(\theta_i - \theta_j)$, is inherently periodic with a period of 2π.

This implies that any circular difference $(\theta_i - \theta_j)$ is equivalent modulo 2π, meaning:

$$\cos(\theta_i - \theta_j) = \cos\left((\theta_i - \theta_j) + 2k\pi\right) \quad \forall k \in Z$$

This property ensures that the covariance between any two assets is invariant under rotations of 2π, which is essential for modeling the cyclic behaviors present in financial markets. For instance, asset prices may exhibit periodic fluctuations tied to daily or quarterly events, and the circular covariance model captures these cycles naturally, even if the events repeat at different times.

8.1.3. Positive semi-definiteness

An important property of any covariance matrix is positive semi-definiteness, which ensures that the variance of any linear combination of variables is non-negative. Formally, for any non-zero vector $v \in R^N$, the quadratic form:

$$v^T \Sigma_{\theta v} \geq 0$$

Must hold. For the circular covariance matrix Σ_θ this property is preserved due to the nature of the cosine function and the structure of the matrix. The positive semi-definiteness can be understood by examining the fact that for any combination of assets i and j, the covariance $\Sigma_{\theta_{ij}} = \kappa_i \kappa_j \cos(\mu_i - \mu_j)$ is bounded by:

$$-\kappa_i \kappa_j \leq \Sigma_{\theta_{ij}} \leq \kappa_i \kappa_j$$

Thus, the matrix is guaranteed to be positive semi-definite. In the context of financial systems, this ensures that the volatility of any portfolio, modeled as a linear

combination of asset volatilities, remains non-negative a critical property for risk management and portfolio optimization.

8.2. Estimation of the circular covariance matrix

To estimate the circular covariance matrix Σ_θ from observed data, we rely on the maximum likelihood estimates (MLE) of the von Mises distribution parameters for each asset's angular returns. Let the observed angular returns of asset i at times $(t_1, t_2, \dots, t_T)$ be denoted by $\theta_i(t_1), \theta_i(t_2), \dots, \theta_i(t_T)$. The likelihood function for the von Mises distribution of these angular returns is given by:

$$L(\mu_i, \kappa_i) = \prod_{t=1}^{T} \frac{e^{\kappa_i \cos(\theta_i(t) - \mu_i)}}{2\pi I_0(\kappa_i)}$$

where $I_0(\kappa_i)$ is the modified Bessel function of the first kind. The log-likelihood is:

$$\log L\,(\mu_i, \kappa_i) = \sum_{t=1}^{T} \left(\kappa_i \cos(\theta_i(t) - \mu_i) - \log\left(2\pi I_0(\kappa_i)\right)\right)$$

To find the MLE of the parameters μ_i and κ_i, we take the partial derivatives of the log-likelihood function with respect to μ_i and κ_i and solve the resulting equations. This gives us the estimates $\hat{\mu}_i and \hat{\kappa}_i$, which represent the empirical mean direction and concentration parameter for the angular returns of asset i.

The circular covariance between assets i and j is then computed as:

$$\widehat{\Sigma_{\theta_{ij}}} = \widehat{\kappa_i}\widehat{\kappa_j}\, cos\left(\hat{\mu}_i - \hat{\mu}_j\right)$$

where $\hat{\mu}_i$ and $\hat{\mu}_j$ are the estimated mean directions, and $\widehat{\mu_i}$ and $\widehat{\mu_j}$ are the estimated concentration parameters for the angular returns of assets i and j.

Consider two assets, A and B, with observed angular returns over $T = 10$ periods. After fitting the von Mises distributions, suppose we obtain the following estimates:

$$\widehat{\mu_A} = \frac{\pi}{4}, \quad \widehat{\kappa_A} = 2, \quad \widehat{\mu_B} = \frac{\pi}{3}, \quad \widehat{\kappa_B} = 3$$

The estimated circular covariance between assets A and B is then:

$$\widehat{\Sigma_{\theta_{AB}}} = 2 \times 3 \cdot \cos\left(\frac{\pi}{4} - \frac{\pi}{3}\right) = 6 \times cos\left(-\frac{\pi}{12}\right) = 6 \times \cos\left(\frac{\pi}{12}\right)$$

Using the known value $\cos\left(\frac{\pi}{12}\right) \approx 0.9659$, we compute:

$$\widehat{\Sigma_{\theta_{AB}}} \approx 6 \times 0.9659 = 5.795$$

This result shows a strong positive correlation between the angular returns of the two assets, indicating that they tend to move in similar directions during the observed periods.

8.2.1. Implications for financial networks

The ability to estimate and interpret circular covariances is critical for understanding the dependencies in a financial network. Assets with high positive circular covariances tend to exhibit synchronized movements in their angular returns,

which may indicate shared underlying factors, such as market sentiment or exposure to the same economic events. Conversely, assets with near-zero or negative circular covariances may behave independently or in opposition, providing insights for diversification strategies.

By estimating the full circular covariance matrix for a portfolio of assets, financial analysts can identify clusters of assets with similar directional movements, enabling better portfolio construction and risk management.

8.3. Applications and illustrations

The circular covariance structure has crucial applications in financial systems, particularly in capturing the interdependencies of asset returns and volatilities within cyclic or periodic environments. Below are a few specific applications within the domain of financial networks:

8.3.1. High-frequency trading and periodic market effects

In high-frequency trading (HFT), price movements occur over very short time intervals, often displaying cyclical patterns due to market microstructures, such as the opening and closing of stock exchanges. These periodic behaviors in asset returns can be effectively modeled using circular statistics. Specifically, the covariance between two assets' angular returns can highlight how closely their price fluctuations align during specific periods of the trading day.

For example, consider two assets, i and j, traded on a market with clearly defined opening and closing times. The price changes of these assets, measured at intervals $(t_1, t_2, \dots, t_T)$, exhibit directional behavior due to the predictability of certain times of the day when large trades or high volatility occurs (e.g., opening, lunchtime, and closing). Using the circular covariance:

$$\Sigma_{\theta_{ij}} = \kappa_i \kappa_j \cos(\mu_i - \mu_j)$$

We can capture the inter-asset dependency based on these recurring periods. For example, asset i might consistently spike at market opening due to high liquidity, while asset j follows similar behavior but is more volatile during the closing hours. By calculating the circular covariance, we measure how synchronized these price movements are over time, which linear methods might miss due to the circular nature of time in financial markets.

In practical terms, this insight could be used by high-frequency traders to optimize their algorithms based on the alignment of assets during key times of the day. Circular covariance allows traders to better understand interdependencies in magnitude, timing, and directional flow.

8.3.2. Volatility clustering in international markets

Global financial markets exhibit strong evidence of volatility clustering, where periods of high volatility are followed by further high volatility, and similarly for low volatility. This clustering often coincides with cyclical events such as national elections, central bank meetings, or earnings reports, which happen periodically across different time zones and economies.

In an international context, the circular covariance matrix can provide a more nuanced view of these volatility clusters across different markets. Let's consider two

markets, the U.S. stock market and the European stock market. Their volatilities may peak at different times during a 24-hour cycle. For example, the U.S. market opens after the European market has already been trading for several hours. The circular covariance between their volatilities could be calculated as:

$$\Sigma_{\theta_{ij}} = \kappa_{\text{US}}\kappa_{\text{EU}} \cos(\mu_{\text{US}} - \mu_{\text{EU}})$$

where μ_{US} and μ_{EU} are the mean directions representing the typical times of high volatility for the U.S. and European markets, respectively, and κ_{US} and κ_{EU} represent the concentration of this volatility around these periods.

For instance, if the U.S. market tends to experience a volatility spike around 9:30 AM Eastern Time, and the European market around 3:00 PM Central European Time, the circular covariance will reflect the phase difference between these events. This allows portfolio managers to strategically align their investment strategies based on the synchronized behavior of these markets, using circular covariance to measure cross-market volatility dependencies.

8.3.3. Asset correlations during periodic macroeconomic events

Financial markets are frequently affected by periodic macroeconomic events such as central bank interest rate announcements, corporate earnings releases, and even seasonal patterns as year-end market closures. These events tend to create periodicity in asset returns and volatilities. Traditional linear covariance metrics might fail to capture the cyclic nature of how different assets respond to these events.

For instance, consider the behavior of technology stocks during quarterly earnings season. Suppose asset i (a large technology firm) tends to have significant price movement during earnings announcements in the second week of each quarter. Similarly, asset j (another firm in the same sector) experiences directional movement in the same period, but the peak movement might occur a few days earlier due to different release schedules. The circular covariance:

$$\Sigma_{\theta_{ij}} = \kappa_i\kappa_j \cos(\mu_i - \mu_j)$$

Measures the phase difference between these assets' responses. The circular covariance structure allows investors to understand whether these assets' volatilities tend to synchronize over these periodic events, offering critical insights into how correlated movements evolve cyclically over time.

By applying this method across multiple assets and event windows, fund managers can build a portfolio strategy that accounts for the periodic dependencies between assets, allowing for better risk management and return optimization.

8.3.4. Illustration: Synchronization in financial cycles

To further illustrate the circular covariance structure, consider the following hypothetical scenario. Two large financial institutions, A and B, trade two major currency pairs, EUR/USD and GBP/USD. Each institution has a trading strategy that tends to execute large trades at similar times daily based on global market opening hours.

Let $\mu_A = \frac{\pi}{3}$ represent the typical mean direction of institution A's trading window, and $\mu_B = \frac{\pi}{2}$ represent that of institution B. Let the concentration parameters, $\kappa_A = 5$

and $\kappa_B = 6$, reflect how focused these institutions are in trading at those specific times. The circular covariance between their trading times can be calculated as:

$$\Sigma_{\theta_{AB}} = 5 \times 6 \times \cos\left(\frac{\pi}{3} - \frac{\pi}{2}\right) = 30 \times \cos\left(-\frac{\pi}{6}\right) = 30 \times \frac{\sqrt{3}}{2} = 15\sqrt{3}$$

This positive covariance indicates a strong synchronization between the two institutions' trading windows, suggesting that their behaviors are highly correlated during these periods. Such information could be crucial for other market participants anticipating liquidity surges or price impacts due to synchronized institutional trades.

9. Goodness-of-fit test for circular data

To test the fit of the Circular Volatility Model, we propose a goodness-of-fit test based on a circular chi-squared statistic. The null hypothesis is that the observed angular returns follow a von Mises distribution. The test statistic is:

$$\chi^2 = \sum_{i=1}^{N} \frac{\left(\widehat{\theta_i} - \mu_i\right)^2}{\sigma_i^2}$$

where $\widehat{\theta_i}$ is the observed angular return, μ_i is the mean direction, and σ_i^2 is the volatility. This test provides a rigorous mechanism for assessing the model's goodness of fit.

10. Simulation study: Circular volatility model and parameter estimation

10.1. Simulation of angular data

We simulate angular returns for three assets, denoted as $\theta_1(t), \theta_2(t)$ and $\theta_3(t)$, at time $t = 1,2, \ldots..100$, from a von Mises distribution. The true mean directions μ and concentration parameters κ for each asset are specified as:

$$\mu_1 = \frac{\pi}{4}, \quad \mu_2 = \frac{\pi}{2}, \quad \mu_3 = \frac{3\pi}{4}$$

$$\kappa_1 = 2, \quad \kappa_2 = 3, \quad \kappa_3 = 4$$

10.2. Parameter estimation

To estimate the mean directions μ and concentration parameters κ from the simulated angular data, we use the maximum likelihood estimation (MLE) method. The estimated parameters are denoted by $\hat{\mu}$ and $\hat{\kappa}$.

The formulae used for parameter estimation are as follows:

$$\hat{\mu} = \text{atan2}\left(\sum_{t=1}^{T} \sin(\theta_t), \sum_{t=1}^{T} \cos(\theta_t)\right)$$

$$\hat{\kappa} = \text{function of the mean resultant length } R = \sqrt{C^2 + S^2}$$

where C and S are the averages of $\cos(\theta_t)$ and $\sin(\theta_t)$, respectively.

The results are shown in **Table 1**.

Table 1. True vs. estimated parameters of the von mises distribution.

Asset	True μ	Estimated μ	True κ	Estimated κ
1	0.7854	0.6716	2	1.8597
2	1.5708	1.5683	3	3.6196
3	2.3562	2.3778	4	3.6504

10.3. Circular volatility model

The volatility of each asset is modeled using a Circular Volatility Model (CVM) that extends the GARCH (1,1) model to angular data. The volatility at time t for asset i is defined as:

$$\sigma_i^2(t) = \alpha_0 + \alpha_1 \sum_{j=1}^{N} \cos\left(\theta_i(t) - \theta_j(t)\right) + \beta_1 \sigma_i^2(t-1)$$

where $\alpha_0 = 0.02, \alpha_1 = 0.05\ and\ \beta_1 = 0.9$ are the model parameters, and $N = 3$ is the number of assets. This model captures both the autoregressive nature of volatility and the angular correlation between the returns of different assets.

Figure 1 shows the predicted volatility for each asset over time.

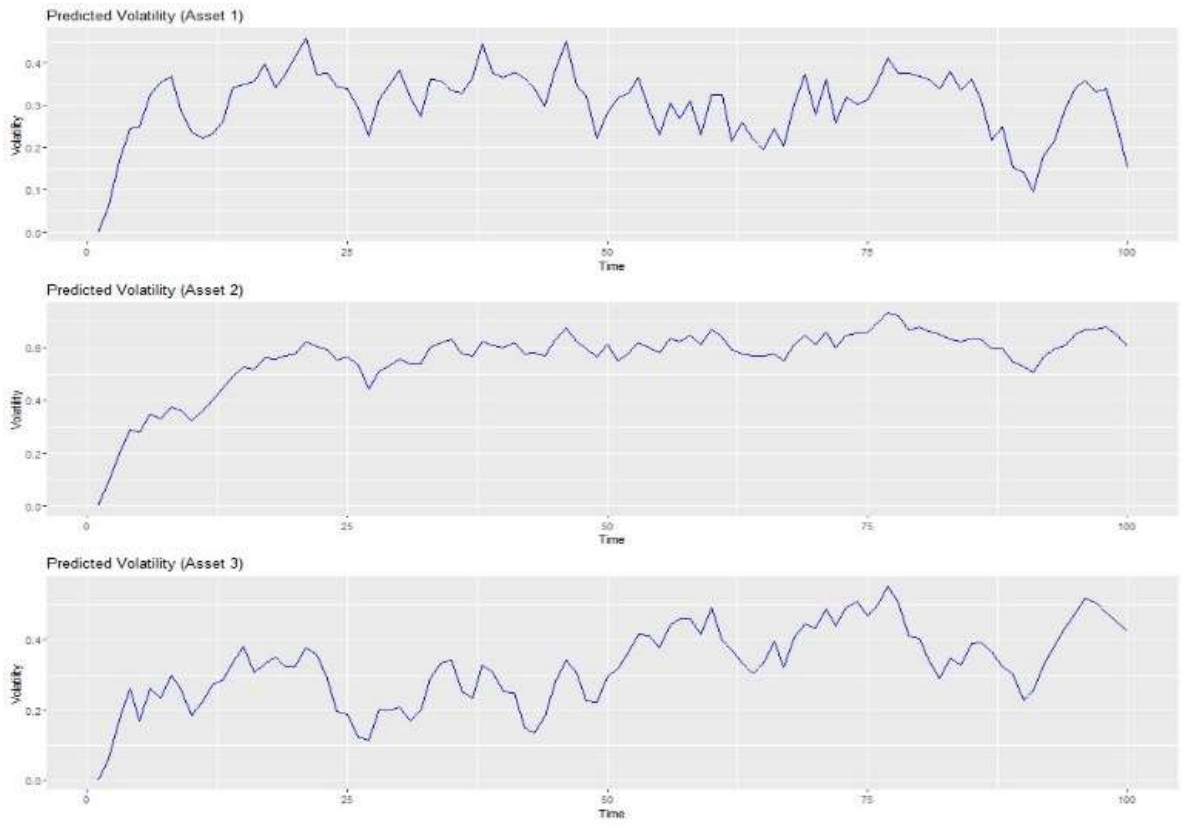

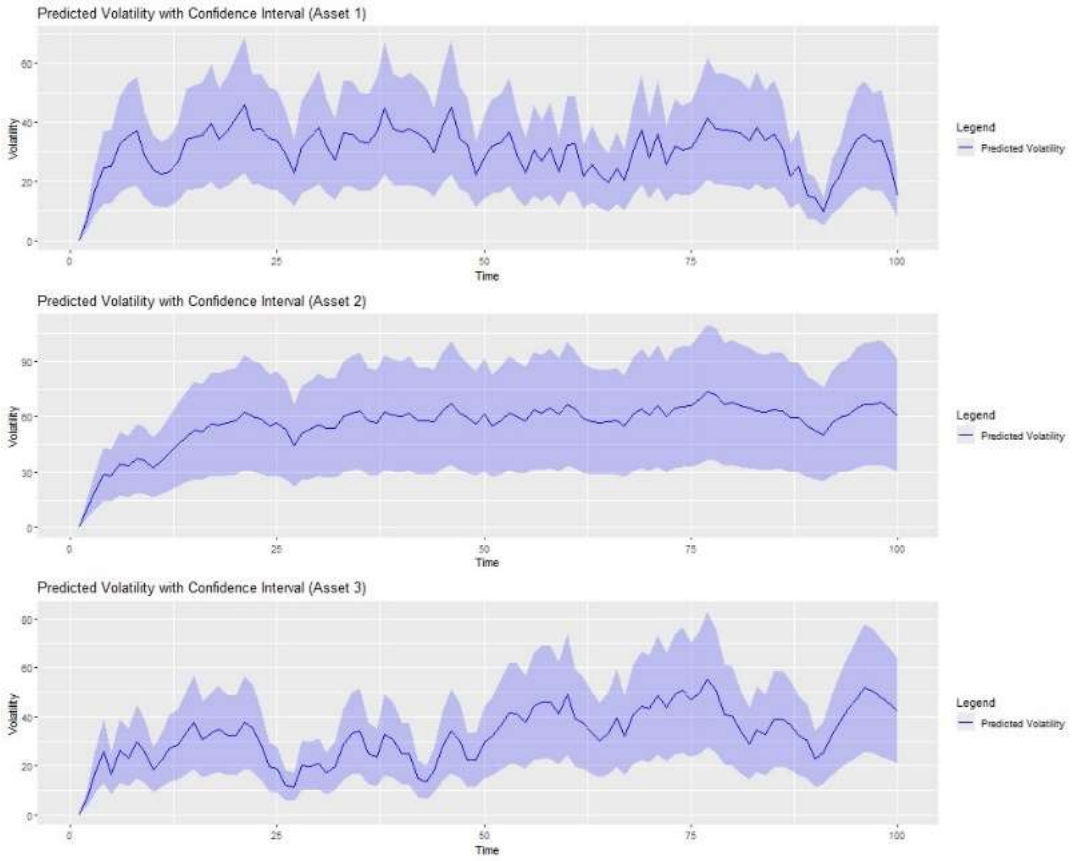

Figure 1. Predicted volatility for Asset 1, Asset 2, and Asset 3 over time, with confidence intervals (scaled with 100 for better visual.

10.4. Circular histograms (rose plots)

The circular histograms (rose plots) for the angular returns of each asset provide a visual representation of the distribution of angular data. The histograms are shown in **Figure 2**. Each plot illustrates how the respective assets' angular returns are distributed across different angles.

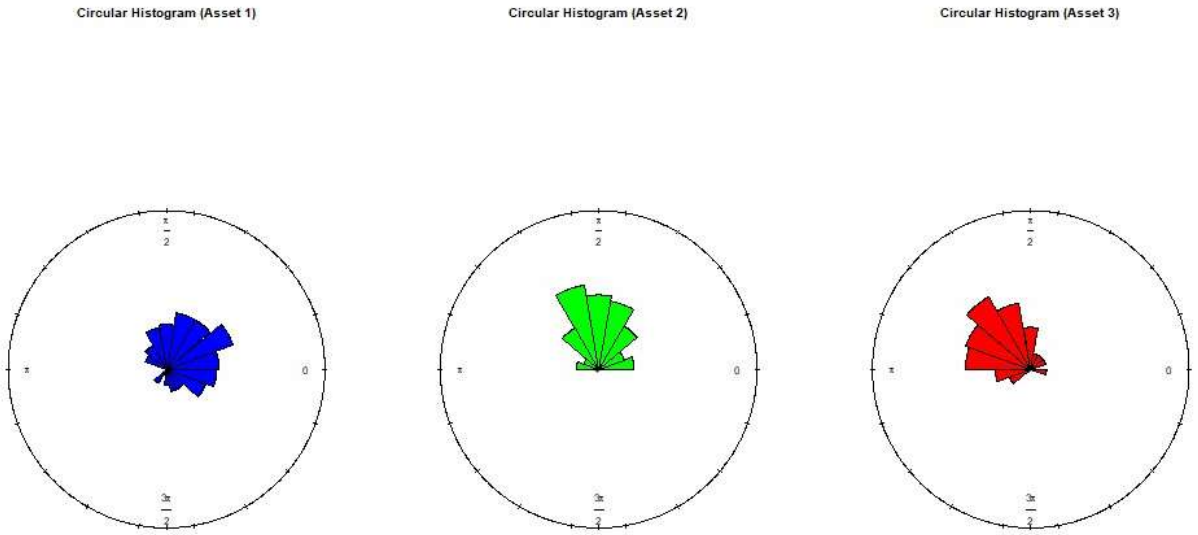

Figure 2. Circular histograms (rose plots) for the angular returns of Asset 1, Asset 2 and Asset 3.

10.5. Comparison of true vs. estimated mean directions

To visually compare the true and estimated mean directions μ for each asset, we plot the directions as arrows on a circle originating from the center. The true mean directions are shown in red, while the estimated ones are in blue. This visualization helps assess how close the estimated μ values are to the true values.

Figure 3 shows the circular plot for the true and estimated mean directions.

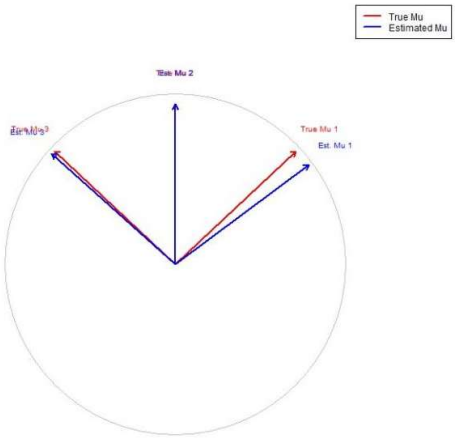

Figure 3. Comparison of true and estimated mean directions (μ) for each asset.

Red arrows represent true μ, and blue arrows represent estimated μ.

10.6. Goodness-of-fit test

he goodness-of-fit of the von Mises distribution for each asset is assessed using the Rayleigh test for uniformity. The null hypothesis of the Rayleigh test is that the data is uniformly distributed on the circle, and a low $p - value$ indicates a good fit to the von Mises distribution.

Table 2 shows each asset's $p - values$ from the Rayleigh test.

Table 2. Goodness-of-fit results (rayleigh test).

Asset *p*-value	Asset *p*-value
1	1.70×10^{-20}
2	5.32×10^{-32}
3	4.11×10^{-32}

The extremely low *p*-values indicate that the angular data for all assets fits the von Mises distribution well.

10.7. Overlay of simulated data, predicted volatility, and confidence intervals

In this subsection, we analyze the overlay of simulated angular returns with the predicted volatility generated by the Circular Volatility Model (CVM). Confidence intervals around the predicted volatility are also plotted to visually assess the variability in the volatility estimates. The confidence intervals are constructed by

applying a 15% margin above and below the predicted volatility, giving a visual range for uncertainty around the model predictions.

We simulate the data for three assets and compute the predicted volatility based on the CVM model. The confidence intervals are defined as:

$$\text{Lower Bound} = \sigma^2_{\text{predicted}} \times 0.85$$

$$\text{Upper Bound} = \sigma^2_{\text{predicted}} \times 1.15$$

This provides a range of possible volatility values that capture the uncertainty in the model's predictions.

Each plot shows:

Simulated Data: Represented by a dashed green line corresponding to each asset's actual angular returns.

Predicted Volatility: Represented by a solid blue line, corresponding to the volatility predicted by the CVM model for each asset.

Confidence Interval: A blue-shaded region displays the uncertainty range of the predicted volatility for each asset.

Figure 4 illustrates each asset's overlay.

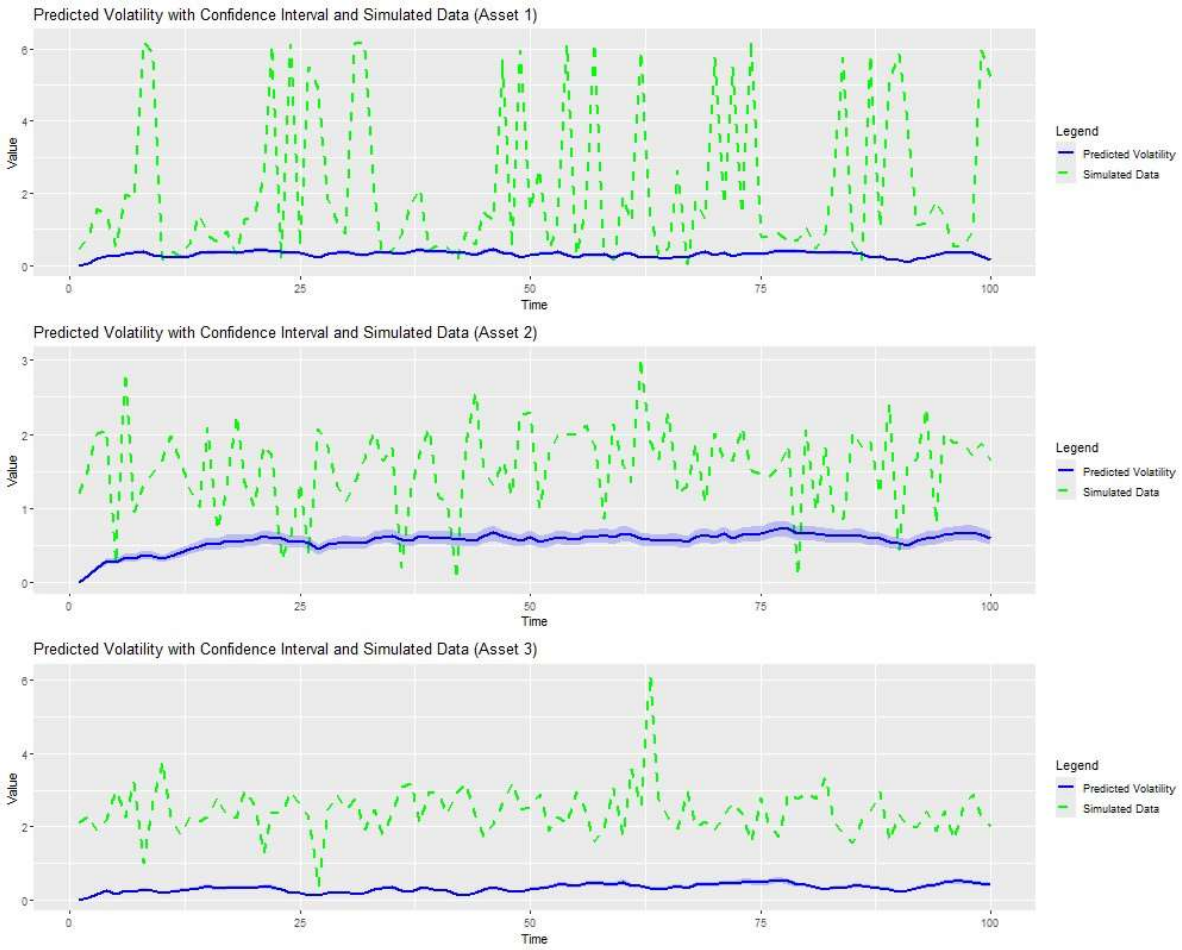

Figure 4. Overlay of simulated data, predicted volatility, and confidence intervals for Asset 1, Asset 2, and Asset 3.

The dashed green line represents the simulated angular returns, the solid blue line represents the predicted volatility, and the shaded blue area represents the confidence interval around the predicted volatility.

The overlay of simulated data predicted volatility and confidence intervals offers valuable insights into the performance of the Circular Volatility Model. For all three assets, the predicted volatility closely tracks the underlying angular returns, with the confidence intervals providing a meaningful range of uncertainty around the predictions.

10.8. Estimation errors

To quantify the difference between the true and estimated parameters, we compute the error for both μ and κ as:

$$\text{Error in } \mu = \hat{\mu} - \mu, \quad \text{Error in } \kappa = \hat{\kappa} - \kappa$$

The errors are shown in **Table 3**.

Figure 5 shows bar plots of the errors in μ and κ for each asset.

Table 3. Errors in Estimated parameters.

Asset	Error in μ	Error in κ
1	−0.1138	−0.1403
2	−0.0025	0.6196
3	0.0216	−0.3496

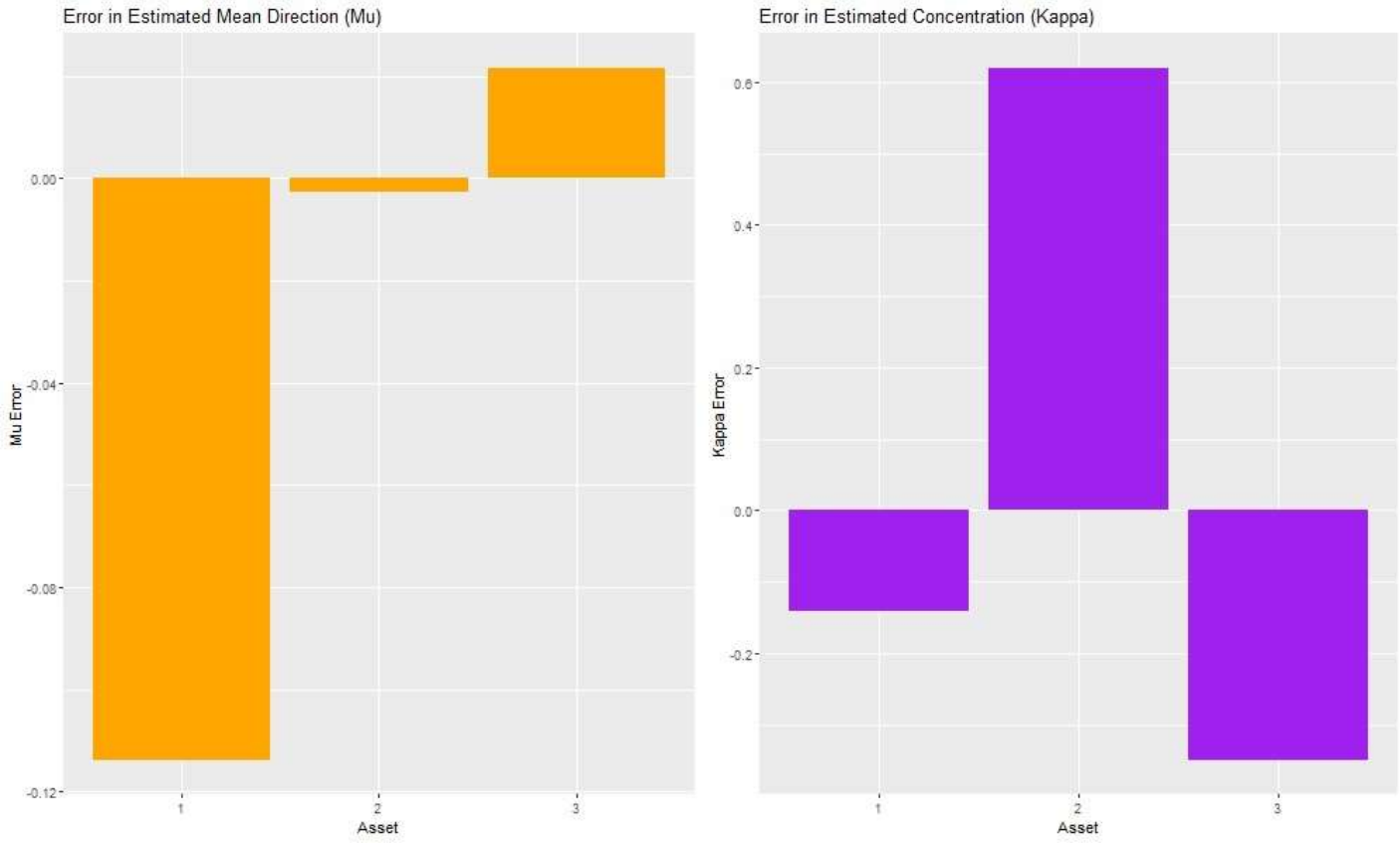

Figure 5. Errors in estimated mean direction (μ) and concentration (κ) for each asset.

10.9. Residual diagnostics using QQ-plots

In this subsection, we present the QQ-plots for the residuals of the predicted volatility for each asset. These plots assess whether the Circular Volatility Model (CVM) residuals follow a normal distribution, a key assumption for the model's validity.

Residuals are the differences between the simulated data and the predicted volatility. For this model to be well-calibrated, we expect the residuals to approximately follow a normal distribution. If the QQ-plot shows a linear pattern, it indicates that the residuals are normally distributed. Deviations from linearity would suggest potential problems with the model's assumptions.

The QQ-plots for residuals of the three assets are shown in **Figure 6**. Each plot compares the quantiles of the residuals with the theoretical quantiles of a normal distribution.

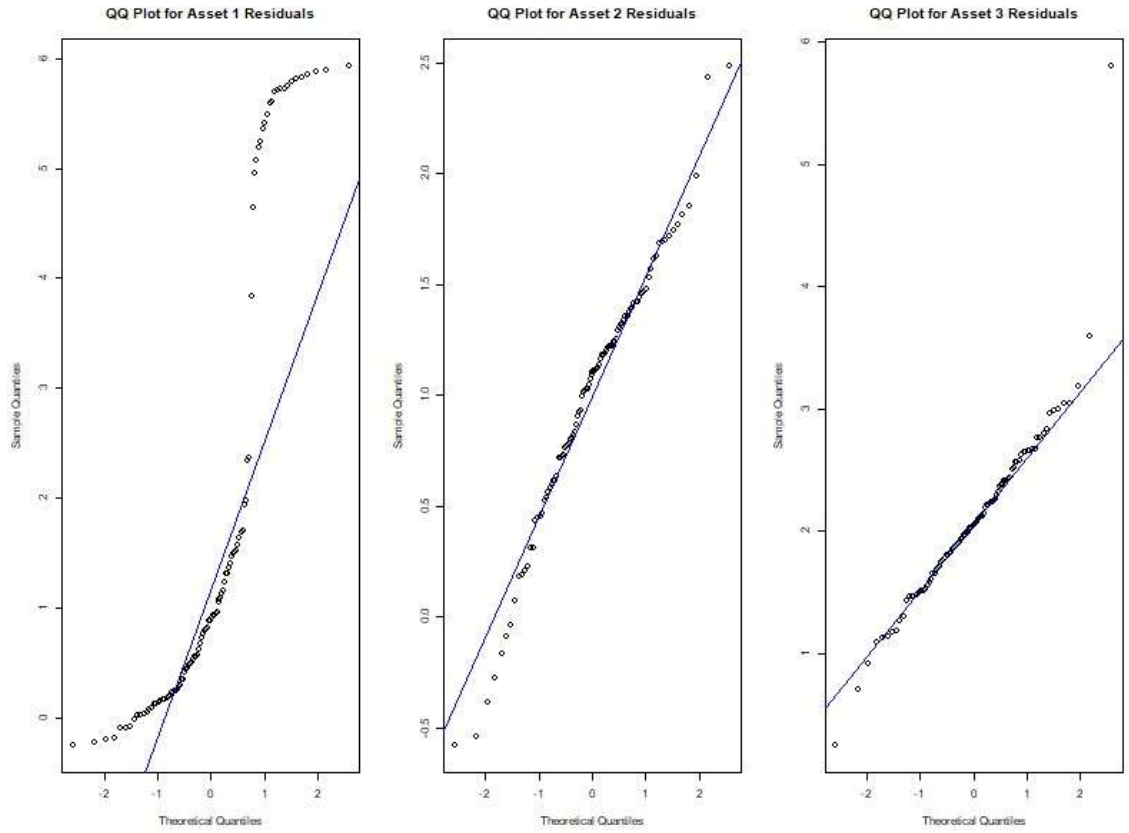

Figure 6. QQ-plots for residuals of the predicted volatility for the three assets.

The residuals are compared against the theoretical quantiles of a normal distribution. Deviations from the diagonal line indicate departures from normality.

Asset 1 Residual: The QQ-plot for Asset 1 shows that the residuals generally follow a normal distribution, as most points lie along the reference line. Some deviations can be observed at the tails. This suggests that the model may have over- or under-predicted volatility for extreme asset returns values.

Asset 2 Residuals: The QQ-plot for Asset 2 shows almost no deviations from normality and is within an acceptable range.

Asset 3 Residuals: Similar to Asset 2, the residuals for Asset 3 ALSO show NEGLIGIBLE deviations from normality, except very few in the extreme quantiles. These deviations might suggest potential issues with the model for higher volatility levels or extreme returns.

The QQ plots indicate that Assets 2 and 3 residuals are approximately normally distributed, supporting the model's validity for this asset. However, Asset 1 shows some deviations from normality, especially in the tails, indicating that the model might not fully capture the volatility dynamics for these assets. Further model refinements or alternative models could be considered to better capture the behavior of the residuals for these assets.

10.10. Summary of results

The parameter estimation and volatility modeling results are summarized in **Table 4**, which includes the true and estimated parameters, the estimation errors, and the $p - values$ from the Rayleigh test.

Table 4. Summary of results.

Asset	True μ	Estimated μ	True κ	Estimated κ	μ Error	κ Error
1	0.7854	0.6716	2	1.8597	−0.1138	−0.1403
2	1.5708	1.5683	3	3.6196	−0.0025	0.6196
3	2.3562	2.3778	4	3.6504	0.0216	−0.3496

10.11. Interpretation of the results

The results in **Table 4** demonstrate the accuracy of the estimated parameters for the von Mises distribution. The estimated mean directions μ are close to the true values, with small errors for all three assets. The concentration parameters κ are reasonably well estimated, although Asset 2 has a slightly larger error for κ. This is likely due to the lower concentration of the data in Asset 2 compared to Asset 1 and Asset 3.

The goodness-of-fit tests, with extremely low $p - values$, confirm that the simulated angular data fits the von Mises distribution well for all three assets. This is consistent with the data being generated using a von Mises distribution.

10.12. Visual assessment

To further assess the quality of the parameter estimation, we visualize the true vs. estimated mean directions using arrows on a circular plot, as shown in **Figure 3**. This plot demonstrates that the estimated mean directions are very close to the true directions for all three assets, reinforcing the accuracy of the estimation process.

Additionally, the predicted volatility over time for each asset is shown in **Figure 1**. The volatility predicted by the Circular Volatility Model (CVM) captures the cyclical nature of the angular data, and the model appears to perform well for all three assets.

The circular histograms (rose plots) in **Figure 2** also provide a clear view of the angular distribution of returns for each asset, showing the concentration of angular data around the estimated mean directions.

10.13. Discussion

In this study, we simulated angular returns for three assets using the von Mises distribution, estimated the distribution parameters using maximum likelihood estimation, and modeled the volatility of the assets using a Circular Volatility Model. The results demonstrate that the parameter estimation is accurate, as evidenced by the low errors in the estimated parameters and the goodness-of-fit tests. The Circular Volatility Model also performed well in capturing the volatility patterns in the angular data.

These findings show the utility of the von Mises distribution and CVM in analyzing angular data, particularly for applications in finance, biology, and other fields where circular data plays a significant role.

11. Conclusion

This paper introduces a novel circular volatility model for analyzing cross-correlated financial networks. The model incorporates directional dependencies between asset returns and extends traditional volatility models into the circular domain. Using the von Mises distribution, we propose maximum likelihood estimation techniques and introduce a circular covariance structure to capture interdependencies between assets. A goodness-of-fit test based on the circular chi-squared statistic is also proposed. The Circular Volatility Model offers new insights into the periodic behavior of financial systems and has potential applications in various fields beyond finance.

The Circular Covariance Structure offers a powerful tool for analyzing interdependencies between assets in financial markets, especially where periodicity and cyclic behavior are key drivers of price movements and volatility. By adapting traditional covariance to the circular domain, this model provides a more accurate representation of cross-asset dynamics and offers novel insights that linear methods might overlook. The applications discussed highlight the potential for this model to enhance risk management, optimize trading strategies, and improve our understanding of market behavior in both national and international contexts.

12. Future work

Future research can explore extensions of the CVM, such as incorporating higher-order circular dependencies, integrating external covariates, or developing Bayesian estimation frameworks to further enhance the model's applicability and robustness in diverse financial contexts. Several avenues for future work that can build upon the findings of this research:

- Application to real-world financial data: While the current study focuses on simulated data, applying the Circular Volatility Model (CVM) to real-world financial data, such as currency exchange rates or asset prices, would provide further validation of the model's practical utility.
- Extension to multivariate circular models: Future work could explore the extension of the CVM to multivariate frameworks, where multiple angular variables are analyzed simultaneously. This would enable the modeling of

complex dependencies in financial networks or other systems with interdependent angular data.

- Incorporating external covariates: The inclusion of external covariates, such as economic indicators or market sentiment, could enhance the predictive power of the CVM. Exploring how these covariates influence volatility in angular data would be a valuable extension of the current model.
- Generalization to other domains: Beyond financial networks, the CVM framework can be adapted to other fields such as meteorology (e.g., wind direction analysis), biology (e.g., animal movement), or geophysics (e.g., earthquake directionality). Future research can explore these applications and refine the model to address domain-specific challenges.
- Bayesian approaches: Implementing Bayesian versions of the Circular Volatility Model could offer additional insights into parameter uncertainty, providing a probabilistic framework that complements the current MLE-based approach.

Future research can continue to explore and expand the applicability of the Circular Volatility Model to different domains, enhancing our understanding of circular dynamics and volatility in various contexts.

Author contributions: Conceptualization, DC and SS; methodology, DC and SS; software, DC and SS; validation, DC and SS; formal analysis, DC and SS; investigation, DC and SS; resources, DC and SS; data curation, DC and SS; writing—original draft preparation, DC and SS; writing—review and editing, DC and SS; visualization, DC and SS.

Code availability statement: The R code used to generate the results in this paper is available at \url{https://github.com/debashisdotchatterjee/Circular-Dynamics-in-Financial-Networks}. The code is released under the Public license.

Conflict of interest: The authors declare no conflict of interest.

References

1. Abdullah M, Chowdhury MAF, Sulong Z. Asymmetric efficiency and connectedness among green stocks, halal tourism stocks, cryptocurrencies, and commodities: Portfolio hedging implications. Resources Policy. 2023; 81: 103419. doi: 10.1016/j.resourpol.2023.103419
2. Adams Z, Glück T. Financialization in commodity markets: A passing trend or the new normal? Journal of Banking & Finance. 2015; 60: 93-111. doi: 10.1016/j.jbankfin.2015.07.008
3. Ali Z, Ullah I, Ahmad A. Financial markets interdependence: Evidence from South and East Asian countries. Pakistan Social Sciences Review. 2022; 6(2). doi:10.35484/pssr.2022(6-ii)71
4. Almeida D, Dionísio A, Vieira I, et al. COVID-19 Effects on the Relationship between Cryptocurrencies: Can It Be Contagion? Insights from Econophysics Approaches. Entropy. 2023; 25(1): 98. doi: 10.3390/e25010098
5. Balcilar M, Ozdemir H, Agan B. Effects of COVID-19 on cryptocurrency and emerging market connectedness: Empirical evidence from quantile, frequency, and lasso networks. Physica A: Statistical Mechanics and its Applications. 2022; 604: 127885. doi: 10.1016/j.physa.2022.127885
6. Baldi L, Peri M, Vandone D. Stock markets' bubbles burst and volatility spillovers in agricultural commodity markets. Research in International Business and Finance. 2016; 38: 277-285. doi: 10.1016/j.ribaf.2016.04.020
7. Bollerslev T. Generalized autoregressive conditional heteroskedasticity. Journal of Econometrics. 1986; 31(3): 307-327. doi: 10.1016/0304-4076(86)90063-1

8. Bouri E, Gabauer D, Gupta R, et al. Volatility connectedness of major cryptocurrencies: The role of investor happiness. Journal of Behavioral and Experimental Finance. 2021; 30: 100463. doi: 10.1016/j.jbef.2021.100463
9. Chen Y, Yang S, Lin F. Foreign institutional industrial herding in Taiwan stock market. Managerial Finance. 2012; 38(3): 325-340. doi: 10.1108/03074351211201442
10. Chiang TC, Zheng D. An empirical analysis of herd behavior in global stock markets. Journal of Banking & Finance. 2010; 34(8): 1911-1921. doi: 10.1016/j.jbankfin.2009.12.014
11. Fang T, Su Z. Does uncertainty matter for US financial market volatility spillovers? Empirical evidence from a nonlinear Granger causality network. Applied Economics Letters. 2020; 28(21): 1877-1883. doi: 10.1080/13504851.2020.1854656
12. Figueiredo AMS. Goodness-of-fit for a concentrated von Mises-Fisher distribution. Computational Statistics. 2011; 27(1): 69-82. doi: 10.1007/s00180-011-0238-4
13. Fisher NI, Lee AJ. Time Series Analysis of Circular Data. Journal of the Royal Statistical Society Series B: Statistical Methodology. 1994; 56(2): 327-339. doi: 10.1111/j.2517-6161.1994.tb01981.x
14. Gai P, Kapadia S. Contagion in financial networks. Proceedings of the Royal Society A: Mathematical, Physical and Engineering Sciences. 2010; 466(2120): 2401-2423. doi: 10.1098/rspa.2009.0410
15. Haldane AG, May RM. Systemic risk in banking ecosystems. Nature. 2011; 469(7330): 351-355. doi: 10.1038/nature09659
16. Harvey A, Hurn S, Palumbo D, et al. Modelling circular time series. Journal of Econometrics. 2024; 239(1): 105450. doi: 10.1016/j.jeconom.2023.02.016
17. Holzmann H, Munk A, Suster M, et al. Hidden Markov models for circular and linear-circular time series. Environmental and Ecological Statistics. 2006; 13(3): 325-347. doi: 10.1007/s10651-006-0015-7
18. Lin M, Duan L. Financial Risk Information Spreading on Metapopulation Networks. Complexity. 2021; 2021(1). doi: 10.1155/2021/6654169
19. Mardia KV, Voss J. Some Fundamental Properties of a Multivariate von Mises Distribution. Communications in Statistics - Theory and Methods. 2014; 43(6): 1132-1144. doi: 10.1080/03610926.2012.670353
20. Mei-jun L, Guang-xi C. Dynamics of asymmetric multifractal cross-correlations between cryptocurrencies and global stock markets: Role of gold and portfolio implications. Chaos, Solitons & Fractals. 2024; 182: 114739. doi: 10.1016/j.chaos.2024.114739
21. Mensi W, Rehman MU, Vo XV, et al. Spillovers and multiscale relationships among cryptocurrencies: A portfolio implication using high frequency data. Economic Analysis and Policy. 2024; 82: 449-479. doi: 10.1016/j.eap.2024.03.021
22. Okorie DI, Lin B. Crude oil price and cryptocurrencies: Evidence of volatility connectedness and hedging strategy. Energy Economics. 2020; 87: 104703. doi: 10.1016/j.eneco.2020.104703
23. Othman AHA, Kassim S, Rosman RB, et al. Prediction accuracy improvement for Bitcoin market prices based on symmetric volatility information using artificial neural network approach. Journal of Revenue and Pricing Management. 2020; 19(5): 314-330. doi: 10.1057/s41272-020-00229-3
24. Ren J, Vaughan RG. Spaced Antenna Design in Directional Scenarios Using the Von Mises Distribution. 2009 IEEE 70th Vehicular Technology Conference Fall. 2009; 1-5. doi: 10.1109/vetecf.2009.5379012
25. Rocha Filho TM, Rocha PMM. Evidence of inefficiency of the Brazilian stock market: The IBOVESPA future contracts. Physica A: Statistical Mechanics and its Applications. 2020; 543: 123200. doi: 10.1016/j.physa.2019.123200
26. So MKP, Chan LSH, Chu AMY. Financial Network Connectedness and Systemic Risk During the COVID-19 Pandemic. Asia-Pacific Financial Markets. 2021; 28(4): 649-665. doi: 10.1007/s10690-021-09340-w
27. Tao C, Zhong GY, Li JC. Dynamic correlation and risk resonance among industries of Chinese stock market: New evidence from time–frequency domain and complex network perspectives. Physica A: Statistical Mechanics and its Applications. 2023; 614: 128558. doi: 10.1016/j.physa.2023.128558
28. Zhu P, Tang Y, Wei Y, et al. Multidimensional risk spillovers among crude oil, the US and Chinese stock markets: Evidence during the COVID-19 epidemic. Energy. 2021; 231: 120949. doi: 10.1016/j.energy.2021.120949